Available online at www.sciencedirect.com

SCIENCE DIRECT

Nuclear Instruments and Methods in Physics Research A 508 (2003) 287–294

NUCLEAR INSTRUMENTS & METHODS IN PHYSICS RESEARCH Section A

www.elsevier.com/locate/nima

Observation of long ionizing tracks with the ICARUS T600 first half-module

F. Arneodo[a], B. Badełek[b], A. Badertscher[c], B. Baiboussinov[d], M. Baldo Ceolin[d], G. Battistoni[e], B. Bekman[f], P. Benetti[g], E. Bernardini[a], M. Bischofberger[c], A. Borio di Tigliole[g], R. Brunetti[g], A. Bueno[c,h], E. Calligarich[g], M. Campanelli[c], C. Carpanese[c], D. Cavalli[e], F. Cavanna[i], P. Cennini[j], S. Centro[d], A. Cesana[k], C. Chen[l], D. Chen[l], D.B. Chen[d], Y. Chen[l], D. Cline[m], Z. Dai[c], C. De Vecchi[g], A. Dabrowska[n], R. Dolfini[g,*], M. Felcini[c], A. Ferrari[j,e], F. Ferri[a], Y. Ge[c], A. Gigli Berzolari[g], I. Gil-Botella[c], K. Graczyk[o], L. Grandi[g], K. He[l], J. Holeczek[f], X. Huang[l], C. Juszczak[o], D. Kiełczewska[b], J. Kisiel[f], T. Kozłowski[p], H. Kuna-Ciskał[q], M. Laffranchi[c], J. Łagoda[b], Z. Li[l], F. Lu[l], J. Ma[l], M. Markiewicz[r], A. Martinez de la Ossa[h], C. Matthey[m], F. Mauri[g], D. Mazza[i], G. Meng[d], M. Messina[c], C. Montanari[g], S. Muraro[e], S. Navas-Concha[c,h], M. Nicoletto[d], G. Nurzia[i], S. Otwinowski[m], Q. Ouyang[l], O. Palamara[a], D. Pascoli[d], L. Periale[s,t], G. Piano Mortari[i], A. Piazzoli[g], P. Picchi[t,u,s], F. Pietropaolo[d], W. Półchłopek[r], T. Rancati[e], A. Rappoldi[g], G.L. Raselli[g], J. Rico[c], E. Rondio[p], M. Rossella[g], A. Rubbia[c], C. Rubbia[g], P. Sala[e,c], D. Scannicchio[g], E. Segreto[i], F. Sergiampietri[v], J. Sobczyk[o], J. Stepaniak[p], M. Szeptycka[p], M. Szleper[p], M. Szarska[n], M. Terrani[k], S. Ventura[d], C. Vignoli[g], H. Wang[m], M. Wójcik[w], J. Woo[m], G. Xu[l], Z. Xu[l], A. Zalewska[n], J. Zalipska[p], C. Zhang[l], Q. Zhang[l], S. Zhen[l], W. Zipper[f]

[a] *INFN - Laboratori Nazionali del Gran Sasso, s.s. 17bis Km 18+910, Assergi (L'Aquila), Italy*
[b] *Institute of Experimental Physics, Warsaw University, Warszawa, Poland*
[c] *Institute for Particle Physics, ETH Hönggerberg, Zürich, Switzerland*
[d] *Dipartimento di Fisica e INFN, Università di Padova, via Marzolo 8, Padova, Italy*
[e] *Dipartimento di Fisica e INFN, Università di Milano, via Celoria 16, Milano, Italy*
[f] *Institute of Physics, University of Silesia, Katowice, Poland*
[g] *Dipartimento di Fisica e INFN, Università di Pavia, via Bassi 6, Pavia, Italy*
[h] *Dpto de Física Teórica y del Cosmos & C.A.F.P.E., Universidad de Granada, Avda. Severo Ochoa s/n, Granada, Spain*
[i] *Dipartimento di Fisica e INFN, Università dell'Aquila, via Vetoio, L'Aquila, Italy*
[j] *CERN, CH-1211 Geneva 23, Switzerland*
[k] *Politecnico di Milano (CESNEF), Università di Milano, via Ponzio 34/3, Milano, Italy*

*Corresponding author. Dipartimento di Fisica, Universita di Pavia, INFN Sezione Sezione di Pavia, via Bassi 6, Pavia I-27100, Italy.

E-mail address: rinaldo.dolfini@pv.infn.it (R. Dolfini).

doi:10.1016/S0168-9002(03)01508-0

[l] IHEP - Academia Sinica, 19 Yuquan Road, Beijing, People's Republic of China
[m] Department of Physics, UCLA Los Angeles, CA 90024, USA
[n] H.Niewodniczański Institute of Nuclear Physics, Kraków, Poland
[o] Institute of Theoretical Physics, Wrocław University, Wrocław, Poland
[p] A.Sołtan Institute for Nuclear Studies, Warszawa, Poland
[q] Institute of Mechanics and Machine Design, Cracow University of Technology, Kraków, Poland
[r] University of Mining and Metallurgy, Kraków, Poland
[s] IFSI - Torino, corso Fiume 4, Torino, Italy
[t] Dipartimento di Fisica, Università di Torino, Via Giuria 1, Torino, Italy
[u] INFN - Laboratori Nazionali di Frascati, Via E. Fermi 40, Frascati (Roma), Italy
[v] INFN - Pisa, via Livornese 1291, San Piero a Grado (Pisa), Italy
[w] Institute of Physics, Jagellonian University, Kraków, Poland

Received 3 February 2003; accepted 7 April 2003

PACS: 29.40

Keywords: Liquid argon; Time-projection chamber; Cosmic rays; Ionization; Muon; Delta rays; Cryogenic detector; Elementary particles

The ICARUS T600 liquid Argon (LAr) detector [1] consists of a large cryostat split in two identical, adjacent half-modules, each of $3.6 \times 3.9 \times 19.9\ \text{m}^3$ internal dimensions. Each half-module (T300) is an independent unit housing an internal detector composed by two Time Projection Chambers (TPCS), a field-shaping system, monitors and probes, and by two arrays of photo-multipliers. Externally the cryostat is surrounded by a set of thermal insulation layers. The TPC wire read-out electronics is located on the top side of the cryostat. The detector layout is completed by a cryogenic plant made of a liquid nitrogen cooling circuit to maintain uniform the LAr temperature, and of a system of LAr purifiers, to keep the LAr purity at a sufficiently high level.

The structure of the internal detector consists of two TPCs per half-module (we refer to as *Left* and *Right* chambers). Each TPC is formed by three parallel planes of wires with gaps of 3 mm. The wires within a plane are parallel and have a pitch of 3 mm between adjacent wires. These planes are named in the following as (1) *induction* plane (wires oriented at 0°), (2) *induction* plane (wires oriented at $+60°$), (3) *collection* plane (wires oriented at $-60°$). The three planes of wires of each TPC are held by a sustaining frame (Fig. 1) positioned onto the longest vertical walls of the

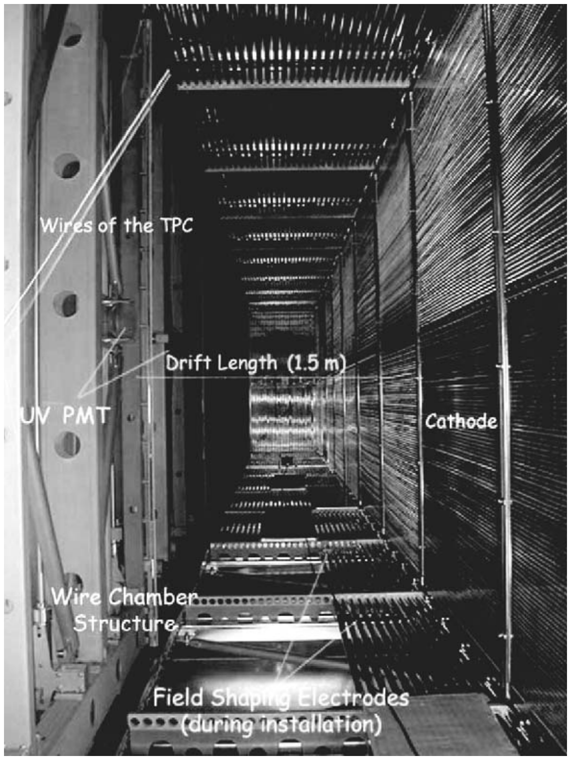

Fig. 1. Picture of the internal detector layout inside the first half-module: the cathode divides the volume in two symmetric sectors. The picture refers to the left sector where wires and mechanical structure of the TPC and some PMTs are visible.

half-module. The total number of wires for each T300 detector is about 27,000. The read-out of the signals induced by ionizing events in LAr on the wires of the TPCs provides means for a full 3D-image reconstruction of the event topology and for an accurate measurement of the energy deposited. A uniform electric drift field perpendicular to the wire planes is established in the LAr volume of each half-module by means of a high voltage system. This is composed by a cathode plane parallel to the wire planes placed in the middle of the LAr volume of each half-module at a distance of about 1.5 m from the wires from both sides, setting to this length the maximum drift path (Fig. 1). The HV system is complemented by field-shaping electrodes to guarantee the uniformity of the field along the drift direction, and by a HV feed-trough to supply the required voltage to the cathode (at a nominal voltage of 75 kV corresponding to 500 V/cm of electric field, the maximum drift time is about 1 ms). The active volume of each half-module delimited by the field-shaping system and the wire planes amounts to $(3.0\,w \times 3.2\,h \times 18.0\,l)\ \mathrm{m}^3$. The active LAr mass is about 237 t in each half-module.

Ionization events in LAr are accompanied by prompt scintillation light emission. The absolute time measurement of the event (T_0) and an internal trigger signal is achieved by detecting this light with an array of PMTs positioned behind the wire planes of each TPC.

The ICARUS electronics is designed to allow continuous read-out, digitization and waveform recording with 2.5 MHz sampling frequency (sampling time of 0.4 μs) of signals from each wire of the TPC. Each of the wire planes of the TPC provides a two-dimensional projection of the event image, where one coordinate is given by the wire position and the other by the drift time. Thus, the various projections have a common coordinate (the drift time). The 3D reconstruction of the event is obtained by correlating signals from two different planes with the help of the common drift coordinate.

The first half-module of the T600 detector has been fully instrumented to allow for a complete test in real experimental condition. The test took place at surface in Pavia (Italy) during the period April–August 2001. The above-ground location of the experimental site allowed the collection of a large sample of cosmic ray events recorded with different trigger configurations. In particular, the coincidence of two scintillator planes suitably positioned provided trigger signals for almost horizontal muon tracks crossing the entire length of the detector (Fig. 2).

Thanks to the unique features of the LAr TPC, fine resolution and high granularity extended over very large active detector mass, the amount of information collected for long tracks is such that an accurate analysis can be performed at the single event level.

Each long muon track is sampled by a large number of wires. The length of the portion of track exposed to a single wire (referred to as the *track pitch length* Δx (cm)) depends on the orientation of the track with respect to the direction of the wires in the plane. The *track pitch length* for each track can be calculated from the 3D reconstruction of the track. For the long muon track sample, they vary between $\Delta x \sim 0.35$–0.40 cm.

By using suitable algorithms applied on the waveform recorded from each wire, one can extract the physical parameters of the individual signal (the "hit") corresponding to the track pitch seen by the current wire. The hit defines the time of drift t_d(μs) and the hit amplitude Q (given in units (ADC×sampling time) as measured by the *collection* plane). The hit amplitude Q corresponds to the ionization charge released by the muon along the track pitch attenuated during the drift by attachment to electro-negative impurities diluted in LAr. The charge attenuation is determined by the level of purity obtained by the LAr purification system and measured by dedicated monitor throughout the data-taking. The purity is expressed in terms of a drift electron lifetime (τ_e) (μs). The "corrected amplitude" Q_cor of the hit is then obtained as

$$Q_\mathrm{cor} = Q\mathrm{e}^{t_\mathrm{d}/\tau_\mathrm{e}}. \qquad (1)$$

This amplitude is proportional to the energy released by the muon along the pitch length. Therefore, the distribution of values $Q_\mathrm{cor}/\Delta x$ from a single muon track reconstruction on the *collection* plane can be directly related to the Landau

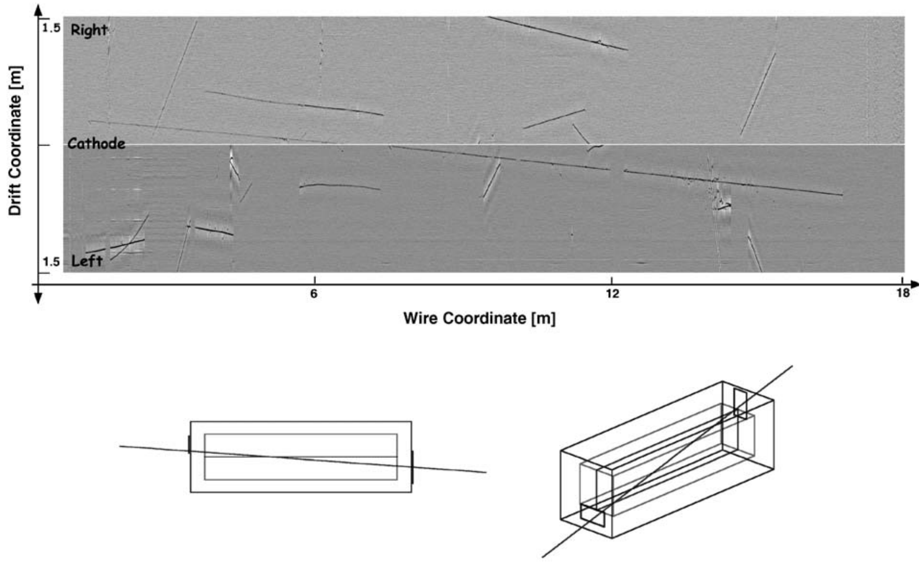

Fig. 2. Run 893, Event 4. (Top) Image of a long-penetrating muon [full (18 m × 1.5 m) collection-left and -right views]: the muon track, triggered by the external scintillator system, is detected first by the right chamber (above) and, after crossing the central cathode, is detected by the left chamber (below). From off-line analysis the event has been reconstructed in space (track length, in the active LAr volume, 18.2 m, absolute orientation $\theta_{\mathrm{Zenith}} = 80.94^\circ$, $\phi_{\mathrm{Azimuth}} = 92.85^\circ$, deposited energy about 4 GeV): (bottom-left) Top view of the T300 detector and the two scintillator layers providing the coincidence trigger; (bottom-right) 3D view of the reconstructed muon track.

distribution of the energy released per unit track length ($\mathrm{d}E/\mathrm{d}x(\mathrm{MeV/cm})$) along the muon track.

In ICARUS, we can take advantage of the very good granularity of the detector to perform a precise estimation of the energy loss by combining the individual charge samplings collected by each wire.

For example, the recorded long muon track in *Run*. 893, *Evt*. 14 (*track pitch length* $\Delta x = 0.395$ cm, measured lifetime $\tau_e = 1570 \pm 133$ μs), is sampled by 2455 *collection* wires. The distribution of $Q_{\mathrm{cor}}/\Delta x$ is shown in Fig. 3. On the same plot, a fit with a convolution of a Landau and a Gaussian function is shown. The Gaussian function describes fluctuations in the measured hit amplitude due to various sources, the main one being electronic noise. The most probable value of the Landau distribution is obtained from the fit:

$$\left(\frac{Q_{\mathrm{cor}}}{\Delta x}\right)_{\mathrm{m.p.}} = 542 \pm 3 \pm 14 \, \frac{\mathrm{ADC} \times \mathrm{sampling\ time}}{\mathrm{cm}} \tag{2}$$

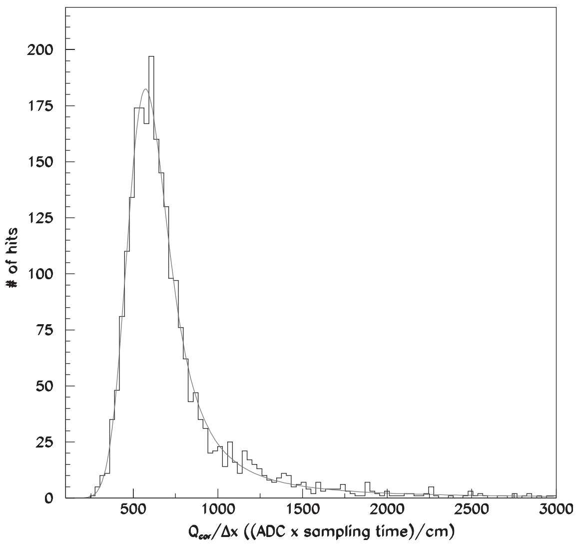

Fig. 3. Distribution of the hit amplitude (drift electron lifetime corrected) per unit of track pitch length (0.4 μs of sampling time) for a single long muon track triggered by the external scintillator system. The continuous line corresponds to the result of a fit with a convolution of a Landau function and a Gaussian function.

where the first term is the statistical error from the fit and the second term corresponds to the systematic uncertainty from the drift electron lifetime correction. The error from the pitch length determination is negligible. We note that the statistical error is smaller than the systematic error because of the very large number of hits collected for a single track.

A number of long muon tracks selected by the external trigger have been analysed using this procedure. The obtained values of $(Q_{\mathrm{cor}}/\Delta x)_{\mathrm{m.p.}}$ were all found to be compatible within errors with the result of Eq. (2).

We now discuss how the precise determination of the most probable energy loss can be readily used to provide an in situ calibration of the detector response.

The range in the detector constraints the momentum of crossing muons above 5 GeV. From a Monte-Carlo simulation of the cosmic muons with appropriate energy and angular distributions, we find that muons crossing the detector and the trigger planes have an average momentum of 28 GeV/c and their effective pitch on the collection wires is $\Delta x \approx 0.4$ cm.

In a dense medium like liquid argon and for the momentum range of interest, the most probable value of the energy loss depends weakly on the particle momentum and on the absorber thickness. Indeed, for the sample of simulated muons that cross the trigger planes, the most probable value of the energy loss per unit track length is

$$\left\langle \frac{\Delta E_{\mathrm{m.p.}}}{\Delta x} \right\rangle_{\mathrm{MC}} = 1.77 \pm 0.02\ \mathrm{MeV/cm}. \qquad (3)$$

From the ratio of Eqs. (3) and (2), we can finally obtain a calibration factor k for the long muon track sample:

$$k = 3.3 \pm 0.1\ \mathrm{keV/(ADC \times sampling\ time)}. \qquad (4)$$

We stress that given the high sampling rate of the energy deposition,this method provides a powerful and reproducible self-calibration of the detector response with excellent accuracy ($\mathcal{O}(\leqslant 43\%)$).

The analysis of very long tracks can be combined to the study of the very short associated tracks (δ-rays produced along the muon track) as shown in Fig. 4. In the figure, one can see how the fine readout granularity allows to record and precisely reconstruct the low-energy tracks down to the MeV range, associated to the large muon event. Indeed, the analysis of δ-rays provides a direct check of the "scaling up" of the LAr TPC by

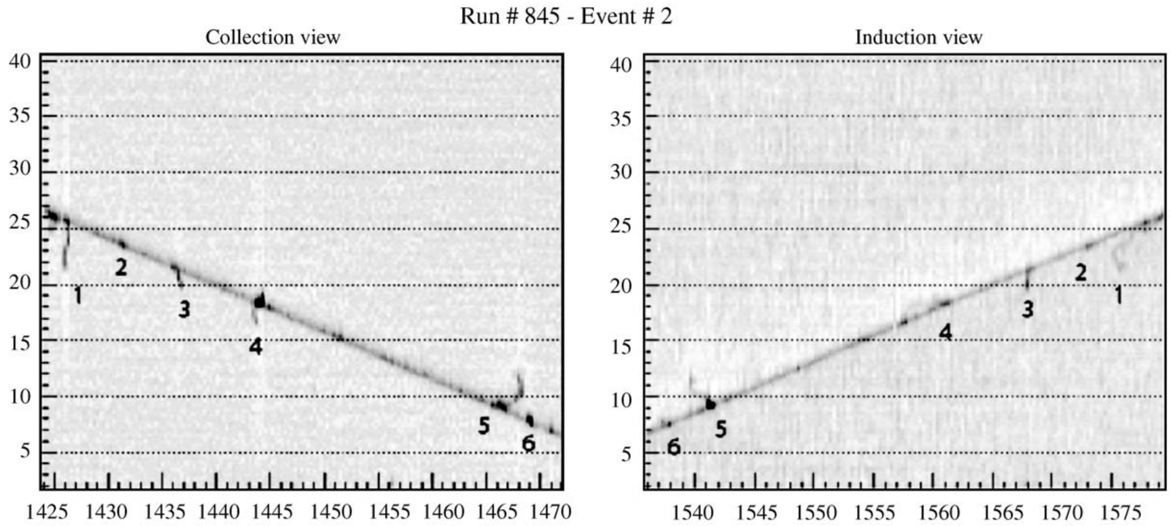

Fig. 4. Example of six δ-rays produced along a segment of a muon track shown in two views (from induction and collection planes). The drift-time axis is the vertical one and the wire coordinate is the horizontal one. Matching points belonging to the same physical event have the same drift-time coordinate.

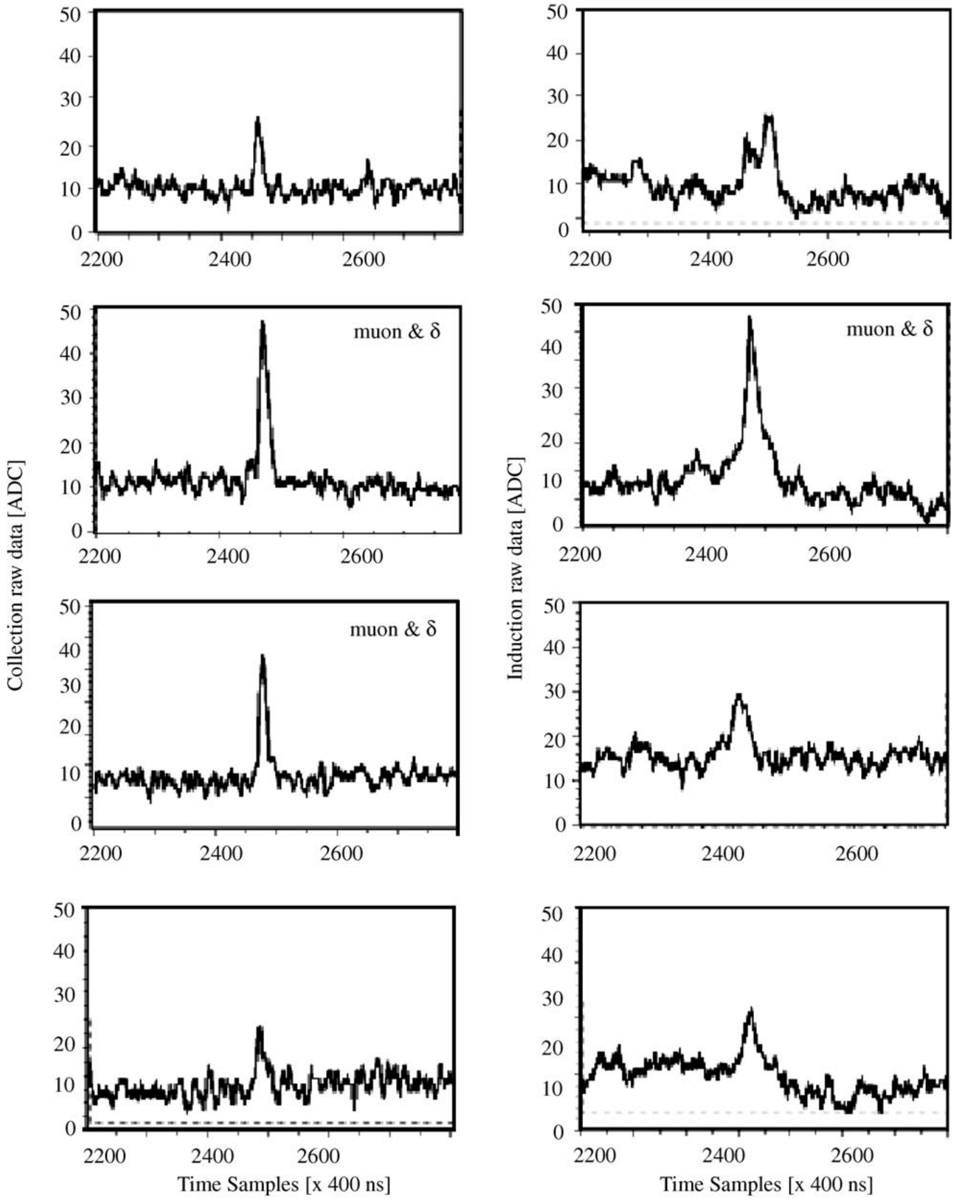

Fig. 5. Signals of four adjacent collection and induction wires showing the presence of a δ-ray in the central wires, where the pulse height is about twice higher with respect to the neighbouring wires due to the presence of the δ-electron emitted parallel to the muon direction.

comparison with similar analyses performed with smaller prototypes [2].

Low-energy δ-rays (i.e. with range shorter than two or three times the wire pitch) cannot be visually resolved from the muon parent track because they tend to be emitted parallel to the muon direction. Nevertheless, they can be recognized through a scanning based on the calorimetric feature of the detector: the muon track is inspected wire by wire, δ-ray counting is incremented and the energy is measured when the charge amplitudes of two or more wires are higher than on adjacent wires by approximately a factor of two. This procedure allows to detect δ-rays with kinetic energy in the range between 1 and 2 MeV. In Fig. 5 signal waveforms from the *collection* and the *induction* planes are shown; the presence of a low-energy δ-ray is detected by comparing the signal amplitudes of neighbouring wires.

When the δ-ray is more energetic (above $\sim$2 MeV), its range exceeds a few consecutive wire pitches and the electron track moves away from the parent muon track due to multiple scattering. Such tracks are easily identified in more than two consecutive wires and in at least two independent views. The track is analysed by computer-aided scanning and the range in space is estimated by means of a 3D track reconstruction obtained by combining drift information with that from at least two of the three wire planes of the TPC. As a result, one identifies the hits belonging to the δ-ray track projection on the different wire planes. As discussed above, each hit corresponding to a segment of the δ-ray projection onto the various planes is individually defined by the wire coordinate, by the drift time coordinate, and by the signal amplitude. A spline fit to the hits positions in one plane (induction) is performed. One can associate the hits of the *collection* plane to the corresponding hit on the *induction* plane by time-projection of the *collection* hits on the spline line. Thus, any pair of associated hits on the two planes, corresponding to the same physical signal (the δ-ray segment in our case) has a common drift-time coordinate. The two wire coordinates of the hit pair together with the drift-time coordinate form triplets of coordinates that can be translated into the Cartesian coordinates of the points belonging to the δ-ray track.

Two methods for the δ-ray energy measurement are employed depending on the δ-ray actual topology, such as unresolved short δ-ray and energetic δ-rays spatially resolved from the parent muon track. In the first case, a calorimetric measurement of the kinetic energy is applied, while in the second one the energy is estimated by range. In the case of the calorimetric measurement, the deposited energy is computed by conversion of the charge collected on the wires into the energy loss of the electron in LAr. The conversion factor is derived by the self-calibration method described above. Obviously, one has to pay attention in subtracting the charge collected from the overlapping muon.

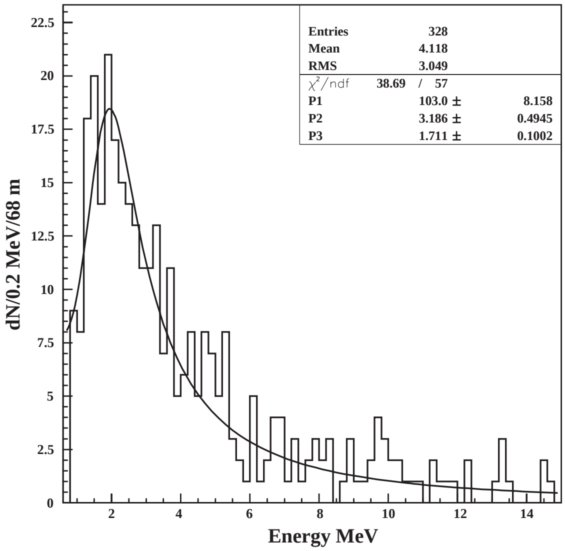

Fig. 6. Distribution of the number of δ-ray/MeV/68 m track. The continuous line represents the result of the fit. The parameter P_3 indicates the actual energy cut-off value estimated by the fitting procedure.

In the second method, the range of electrons in LAr is converted into energy [3], as computed by NIST tables [4] under continuous slowing down approximation. Few long muon tracks for a total length of 68 m have been analyzed and a total of 328 δ-rays were selected. Their energy has been individually measured following the two methods described above. The measured rate corresponds to about 4.8 δ-rays/m. The corresponding energy spectrum is shown in Fig. 6. The simplified Mott formula [5] for elastic scattering of electrons by the Coulomb field of a charged particle in the system in which the electron is initially at rest can be modified to account for the selection efficiency, obtaining

$$\frac{d^2N}{dx\,dT} = \left[P_1 \frac{1}{1+e^{-P_2(T-P_3)}}\right]\frac{1}{\beta^2}\frac{1}{T^2} \qquad (5)$$

where $d^2N/dx\,dT$ is the rate of δ-rays per unit muon track length with electron kinetic energy in the interval between T and $T + dT$.

The sigmoid function used in (5) to account for the geometrical efficiency and the efficiency of the event selection at low energy depends on three parameters: the abscissa P_3 at the flex point representing the actual energy cut-off value, the slope P_2 of the sigmoid function at the flex point and a normalization factor P_1. The continuous line in Fig. 6 represents the fit to the data with Eq. (5). The fitted kinetic energy cut-off value is found to be 1.7 ± 0.1 MeV. The result shows agreement between data and predictions. Accounting for the different cut-off values and geometrical efficiency of the detector, these results agree with those obtained with the 50-l ICARUS prototype [2].

To conclude, in 2001 a major milestone has been achieved: the first module of the ICARUS T600 detector has been successfully tested at surface. In this letter, we have illustrated the unique features of the LAr TPC, namely the fine resolution and high granularity extended over very large active detector masses, with the simultaneous calorimetric and imaging reconstruction of up to 18 m long muon tracks and short associated δ-ray tracks. This demonstrates that the scaling-up in volume to the full-size detector has been successfully achieved, opening the way to the possibility of carrying out the proposed physics program after commissioning of the first T600 detector at the Gran Sasso Laboratory.

We would like to warmly thank the many technical collaborators that contributed to the construction of the detector and to its operation. We are glad of the financial and technical support of our funding agencies and in particular of the Istituto Nazionale di Fisica Nucleare (INFN), of ETH Zürich and of the Fonds National Suisse de la Recherche Scientifique, Switzerland. The Polish groups acknowledge the support of the State Committee for Scientific Research in Poland, 2P03B09520, 2P03B13622; the INFN, FAI program; the North Atlantic Treaty Organization, linkage grant PST.CLG.977410; the EU Commission, TARI-HPRI-CT-2001-00149.

References

[1] P. Cennini, et al. (The ICARUS Collaboration), A first 600 t ICARUS detector installed at Gran sasso Laboratory, Addendum to ICARUS Proposal, LNGS 95/10, 1995.

[2] F. Arneodo, et al., (The ICARUS Collaboration), Nucl. Instr. and Meth. A 449 (2000) 42.

[3] S. Goudsmit, J.L. Saunderson, Phys. Rev. 57 (1940) 24.

[4] National Institute of Standards and Technology, Web site: http://www.nist.gov/.

[5] N.F. Mott, Proc. Roy. Soc. 124 (1929) 425;
H.L. Bradt, B. Peters, Phys. Rev. 74 (1948) 1828.